Magnetic-field-enhanced forbidden modes in Co-doped ZnO thin films revealed by Raman scattering

J. T. Ji,[1,2] A. M. Zhang,[1] T. L. Xia,[1] Q. Cao,[3] G. L. Liu,[3] D. Hou,[3] and Q. M. Zhang[1,2,*]

[1]*National Laboratory of Solid State Microstructures, Department of Physics, Nanjing University, Nanjing 210093, People's Republic of China*

[2]*Department of Physics, Renmin University of China, Beijing 100872, People's Republic of China*

[3]*School of Physics and Microelectronics, Shandong University, Jinan 250100, People's Republic of China*

(Received 14 June 2010; published 12 July 2010)

We have performed Raman-scattering measurements on single-crystalline ZnO thin films with 0 and 3% Co doping. In the 3% Co-doped sample, three additional peaks are found whose intensities grow rapidly with applied magnetic fields up to 7 T, and which remain even at room temperature. The nature of the "forbidden" modes is explained in terms of bound magnetic polarons (BMPs), whose electronic density around each Co^{2+} impurity is altered by the field. This implies that BMPs dominate the local properties of dilute magnetic semiconductors (DMSs) at low-carrier concentrations, and further that they may play an important role in mediating long-range magnetic order.

DOI: 10.1103/PhysRevB.82.014408 PACS number(s): 78.30.Fs, 63.20.−e, 75.50.Pp, 78.20.Ls

DMSs exhibit a number of unique magneto-optical and magneto-electric properties, which arise from the interaction between the carriers and the magnetic ions. In particular, the high-spin-injection efficiencies they permit make them key candidate materials for future spintronics applications. Considerable effort has been expended in the search for DMSs with high Curie temperatures (T_c), and in this context ZnO-based systems have attracted much attention. While the predicted[1,2] room-temperature ferromagnetism has indeed been observed in Co-doped ZnO thin films,[3] the question of whether the ferromagnetic signal is intrinsic or arises only from the magnetic impurities remains controversial.[4–6]

Several theoretical models have been proposed to understand long-range magnetic order in DMSs. The Ruderman-Kittel-Kasuya-Yosida (RKKY) model, developed for interactions between local *f*-electron spins mediated by itinerant *s* electrons, is not appropriate in DMSs because of the weaker localization of their *d* electrons.[7] A modified Zener model incorporating some of the same ideas, and valid for higher carrier concentrations, provided predictions valuable in the search for high-T_c DMSs.[1] First-principles calculations suggest a double-exchange model where interactions are mediated by itinerant electrons instead of oxygen ions,[2] and again higher carrier concentrations are required. In a magnetic-polaron theory,[8] carriers from intrinsic hydrogenic impurities, which arise from vacancies and interstitials whose concentration[9] is of order 10^{18} cm^{-3}, interact with and polarize the magnetic ions within their effective radius to form BMPs. Long-range ferromagnetism emerges as these magnetic clusters overlap, which accounts for the observation of ferromagnetism also at low carrier concentrations. The different models are supported to a greater or lesser extent by different measurements, and to date there is no consensus on ferromagnetism in DMSs. There is, thus, a pressing need for specially designed experiments able to obtain the information critical for understanding the mechanism.

Raman scattering is a unique technique for the investigation of electronic and magnetic excitations, and has been used widely for exploring lattice vibrations and impurity phases in DMSs. We have performed Raman-scattering measurements over a range of temperatures and fields on single-crystalline ZnO thin films selected carefully to ensure that the features observed are truly intrinsic. We find in Co-doped ZnO films that an applied magnetic field causes a very significant enhancement of three forbidden phonon excitations, which we determined to be B_1 and its second-order modes. Comparison of the Raman spectra for different doping concentrations, temperatures, and magnetic fields leads unavoidably to an explanation in term of BMPs. Our results therefore confirm that BMPs indeed exist in low-carrier-concentration DMSs and that they have a dominant effect on local magnetic properties, while in addition suggesting strongly that their overlap may be key to the emergence of long-range magnetic order.

ZnO:Co thin films were grown by a radio-frequency oxygen plasma-assisted molecular beam epitaxy (MBE) process. High-purity 6N Zn, 5N Co, and 5.5N O_2 sources were used. A 30 nm ZnO buffer layer was deposited on an Al_2O_3 (0001) substrate, followed by a 100 nm ZnO:Co epilayer with a growth rate of 0.9 nm/min at 450 °C. The presence of single-crystalline phases was confirmed by real-time reflection high-energy electron diffraction (RHEED) and by high-resolution x-ray diffraction. The Co concentration was controlled through the ratio of Zn and Co fluxes and verified by *in situ* x-ray photoelectron spectroscopy (XPS) and energy-dispersive x-ray analysis (EDX). The XPS spectra indicate that Co^{2+} ions have been incorporated into the host lattice at the Zn^{2+} sites. More details concerning thin-film growth and characterization may be found in Ref. 10.

We present first our magnetization measurements on pure and 3% Co-doped samples, which were made with a quantum design superconducting quantum interference device (SQUID). The measurements, shown in Fig. 1, were performed at room temperature. While there is no discernible hysteresis in a ZnO film, a hysteresis loop is clearly visible for the 3% Co-doped sample. This demonstrates that long-range ferromagnetic order is present, and that it persists to temperatures of 300 K.

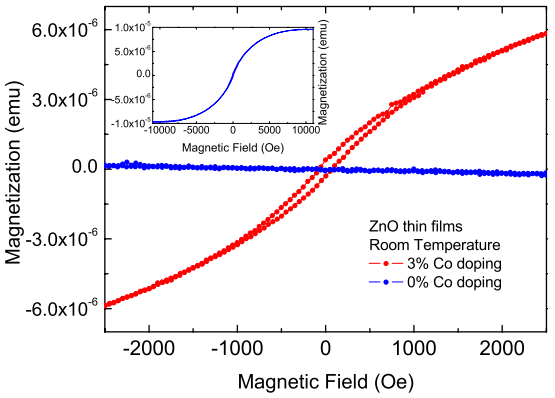

FIG. 1. (Color online) Magnetization as a function of field for pure and 3% Co-doped ZnO thin films at room temperature. Inset: magnetization over a wider field range.

The Raman measurements were performed with a triple-grating monochromator (Jobin Yvon T64000) whose resolution is 0.6 cm^{-1} (subtractive mode). A 50× objective microscopic lens with a working distance of 10.6 mm was used to focus the incident light on the sample and to collect the scattered light. The detector is a back-illuminated charge-coupled device (CCD) cooled by liquid nitrogen. The laser beam, of wavelength 532 nm and approximate power 3 mW, was focused into a spot of diameter *ca.* 5 μm on the sample surface. The samples were mounted in a helium cryostat under a vacuum of 10^{-7} torr and the magnetic field was applied using a superconducting magnet (Cryomagnetics) with a room-temperature bore.

ZnO is a polar crystal and possesses a wurtzite structure with point group C_{6V}^4, both the Zn and O atoms occupying C_{3V} sites. This symmetry allows $A_1+E_1+2E_2$ Raman-active modes and silent B_1 modes. The Raman-active modes have been assigned and studied in many previous measurements.[11] Fig. 2 shows the zero-field Raman spectra for pure and 3% Co-doped thin films from 8 to 300 K. The peaks located at approximately 100, 380, 437, and 582 cm^{-1} in Fig. 2(a) can

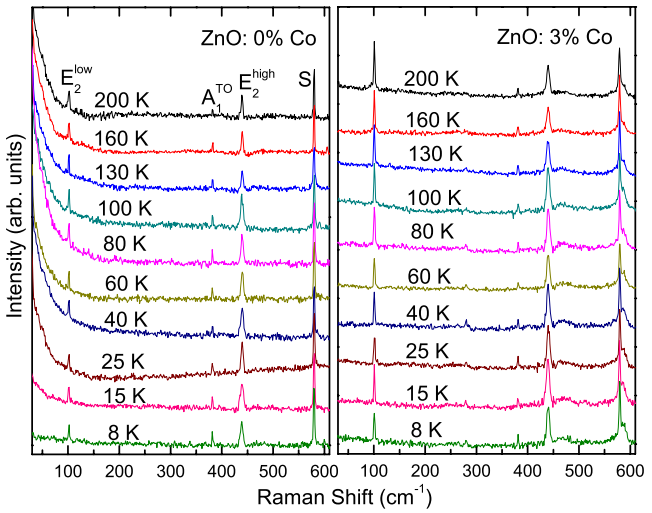

FIG. 2. (Color online) Raman spectra of pure and 3% Co-doped ZnO thin films over a range of selected temperatures.

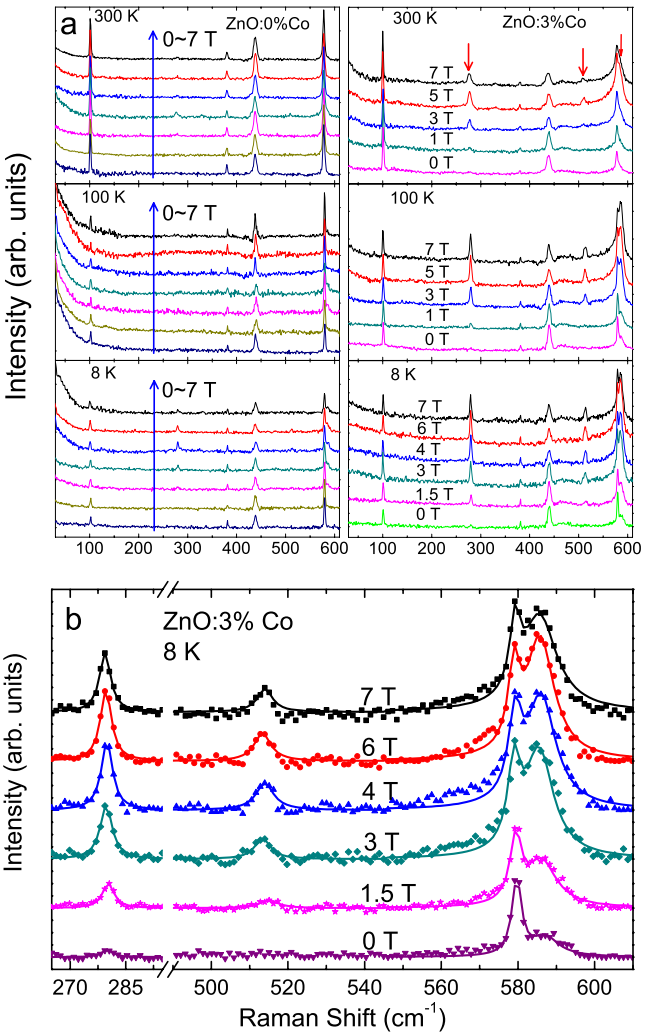

FIG. 3. (Color online) (a) Raman spectra of pure (left) and 3% Co-doped (right) ZnO thin films at three temperatures and for a range of fields. Red arrows indicate the enhanced modes. (b) Magnified spectra of 3% Co-doped ZnO, shown for the strongly field-enhanced peaks at 278, 512, and 586 cm^{-1} at 8 K for different applied magnetic fields. Symbols denote experimental data and curves denote Lorentzian fits.

be assigned, respectively, to the modes E_2^{low}, $A_1(TO)$, E_2^{high}, and the E_g mode (S in Fig. 2) of the sapphire substrate.[16] These modes also dominate the spectra of the 3% Co-doped system [Fig. 2(b)], but weak additional peaks are discernible at approximately 278 and 586 cm^{-1}, and a very weak peak at 512 cm^{-1}.

The primary focus of this manuscript is the magnetic field dependence of these additional peaks. In the Raman spectra shown in Fig. 3(a) for the two samples at 8, 100, and 300 K, the results for pure ZnO show no obvious or systematic change due to the magnetic field; we comment below on the weak enhancement of the 278 and 586 cm^{-1} modes apparent only at intermediate (but not at high) fields. By contrast, in the 3% Co-doped sample there is an unambiguous and dramatic enhancement of the three additional peaks mentioned above. This enhancement increases with the field and increases with decreasing temperature. Figure 3(b) shows the 8

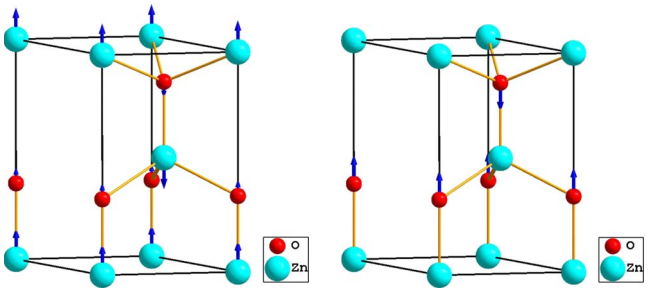

FIG. 4. (Color online) Representation of atomic vibrational motion in the silent B_1 modes. Left: B_1^{low}. Right: B_1^{high}.

K spectra of the Co-doped sample in detail for the frequencies corresponding to these peaks.

To understand this strong, field-induced enhancement of the three forbidden modes, first their origin must be established. These modes have in fact been observed in N-substituted ZnO, where they were thought to be induced by the N impurities,[12] but were later reported also in samples with nonisoelectronic cation substitution.[13] By combining the available experimental evidence with first-principles calculations, these features were determined[14] to be the silent B_1 plus its second-order modes, which usually appear simultaneously as a characteristic fingerprint (Fig. 4). In detail, the peaks at 278, 512, and 586 cm^{-1} correspond, respectively, to the B_1^{low} vibration of Zn along the c axis, the second-order $2B_1^{\text{low}}$ mode, and the B_1^{high} vibrational mode of O along the c axis. A schematic representation of the B_1 modes is presented in Fig. 5. The appearance of the silent modes at zero field [Fig. 3(b)], albeit with very low intensity, suggests that their activation is caused by the breaking of local translational symmetry due to Co^{2+} impurities, which lifts the constraint of momentum conservation.[13,14] Breaking of translational symmetry at the interface of the thin film could in principle also allow the (weak) presence of these modes both with and without Co-doping,[21] a topic to which we return below.

For a quantitative analysis of the enhancement effect, the solid lines in Fig. 3(b) are Lorentzian fits to the intensities of the three forbidden modes. Taking into account the intensity fluctuations caused by temperature changes and by laser power drift, it is more appropriate to compare the relative intensities: from the fit we take the relative integrated intensities normalized by the substrate (582 cm^{-1}) mode in the same spectrum. The dependence of the relative intensity on magnetic field at different temperatures is shown in Fig. 5. The intensities of the three "forbidden" modes show a clear and almost linear increase with magnetic field up to 5 T, beyond which the slope decreases toward a saturation of the enhancement effect.

This unique and unambiguous enhancement places strict constraints on any microscopic explanation. First, the effect has no connection to magnetic excitations (magnons or other spin-flip processes), which would have an energy shift linear in the applied field, as well as much lower mode energies. Second, the field-induced enhancement of an infrared-active phonon mode was reported in α-Al_2O_3 and interpreted as a change of polaron cyclotron mass.[15] However, because the isovalent substitution of Co^{2+} ions at low concentrations has

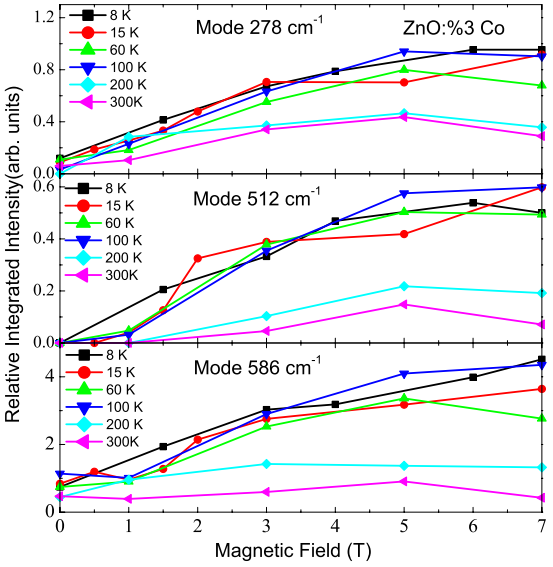

FIG. 5. (Color online) Magnetic field dependence of relative Raman intensities of the three enhanced peaks, normalized to the intensities of the respective substrate (582 cm^{-1}) modes.

little effect on the electron-phonon coupling, a polaron scenario cannot explain why the forbidden modes are enhanced only in the doped sample. Third, the latter problem applies also to a carrier-mediated mechanism for ferromagnetism, such as RKKY or double exchange. We stress again that our samples have only a low-carrier concentration, with no extrinsic carrier doping. Finally, a similar enhancement by external magnetic field was reported in both doped and undoped $GaAs/Al_xGa_{1-x}As$ superlattices,[21] where it was explained as confined LO phonons and interface modes. The present results differ fundamentally from those obtained for superlattices, in that the systematic and quasilinear enhancement effect exists only in the Co-doped ZnO sample, and thus cannot be ascribed to an interface effect. However, the weak intensities of the forbidden modes visible at some fields in the undoped ZnO thin film [Fig. 3(a)] may be attributed to the interface.

Returning to Fig. 3(b), the very low intensity of the forbidden modes at zero field indicates that the isovalent Co^{2+} ions only have a small effect on the host lattice. However, by comparison with the N- and cation-substitution[13] experiments mentioned above, the effect of an applied magnetic field is to cause the Co^{2+} ions to act in a manner similar to such impurities. This implies immediately that an applied magnetic field must affect the electronic configuration of Co^{2+} ions, i.e., that it must cause a transfer of electron density within the $3d$ orbitals.

Such a transfer may be understood naturally in the BMP picture. In a BMP, the s-d exchange between a local spin $\vec{S}$ and a donor electron spin $\vec{s}$ can be represented by an effective molecular field $H_W = J_{sd}\langle S_z\rangle / 2\mu_0\mu_B\rho^3$, where J_{sd} is the s-d exchange parameter, $\langle S_z\rangle$ is the average z component of the local spin $\vec{S}$, μ_0 is the magnetic susceptibility in vacuum, μ_B is the Bohr magneton, and $\rho = r_H / r_c$ is the ratio of the hydrogenic orbit radius of a donor electron to the cation radius.[8] Typical values of 1.5 eV for J_{sd}, 3/2 for $\langle S_z\rangle$, and 13

for ρ yield an estimate for the effective molecular field of approximately 8 T, comparable to the maximum applied field. The applied field can be considered equivalent to an increase in effective *s-d* exchange energy, and hence controls the transfer of electronic density in a BMP. Coey *et al.* suggest further that this electron density transfer causes an effective enlargement of r_c, which is important in the explanation of high-T_c ferromagnetism in DMSs.[8]

A quantitative analysis based on this microscopic description follows the bond-polarizability model of Wolkenstein,[17] which has been applied extensively to calculate Raman intensities. The dominant contribution to the electronic polarizability is taken to be from pairs of nearest-neighbor atoms, and can be written as[18]

$$\alpha_{ij} = \frac{1}{3}(2\alpha_p + \alpha_l)\delta_{ij} + (\alpha_p - \alpha_l)\left(\frac{1}{3}\delta_{ij} - \frac{r_i r_j}{r^2}\right), \quad (1)$$

where $\vec{r}$ is the connecting vector of a pair. α_p and α_l are, respectively, the perpendicular and longitudinal bond polarizabilities. Taking a spherical ionic shell and including the effect of induced ionic dipoles, one obtains[19]

$$\alpha_p = 4\pi\epsilon_0\left[\left(\frac{1}{r_c^3} + \frac{1}{r^3}\right)^{-1} + \left(\frac{1}{r_a^3} + \frac{1}{r^3}\right)^{-1}\right], \quad (2)$$

$$\alpha_l = 4\pi\epsilon_0\left[\left(\frac{1}{r_c^3} - \frac{2}{r^3}\right)^{-1} + \left(\frac{1}{r_a^3} - \frac{2}{r^3}\right)^{-1}\right], \quad (3)$$

in which $r_c(r_a)$ is the cation (anion) radius and the bond length is $r=r_c+r_a+x$. For a Co-O bond oriented along the c axis in ZnO, the derivative of the polarizability with respect to the c-axis displacement x of Co is[18]

$$\frac{\partial\alpha}{\partial x} = \frac{\partial\alpha_l}{\partial r} = -24\pi\epsilon_0 r^2\left[\left(\frac{r^3}{r_c^3} - 2\right)^{-2} + \left(\frac{r^3}{r_a^3} - 2\right)^{-2}\right]. \quad (4)$$

The Raman intensity is in general proportional to the square of the induced polarizability derivative, $I \propto (\partial\alpha/\partial x)^2$.[20] Analysis of the forbidden modes requires only the cation polarizability and the magnetic field dependence of r_c. Based on the above formulas and considering the approximately constant ratio of r_a to r_c, one obtains $\partial\alpha/\partial x \propto r_c^2$. Thus $I \propto r_c^4$, and hence $I \propto H^{4/3}$.[8] This result agrees well with the behavior of the measured Raman intensity in the regime below 5 T, as illustrated in Fig. 5. The transfer of electronic density in an applied field is limited by the fact that the local Coulomb energy is driven up, which results in the saturation above 5 T.

In summary, we have performed Raman-scattering measurements over a range of temperatures and magnetic fields on high quality, single-crystalline ZnO:Co thin films. In 3% Co-doped samples, the forbidden B_1 single and multi-phonon modes show a dramatic enhancement due to the magnetic field. This result places strict constraints on valid microscopic models: the BMP framework provides both a natural qualitative interpretation and a quantitative description of the experimentally determined field dependence of the Raman intensity.

These observations shed further light on the question of ferromagnetism in DMSs, and prove that phonon enhancement in a magnetic field is a very sensitive and quite unique probe of these systems. Our Raman measurements demonstrate not only the existence of BMPs in low-carrier-concentration DMSs, but that they dominate the local magnetic properties. Given our observation of a ferromagnetic hysteresis loop, and the persistence of the field-induced mode enhancement, at room temperature in the Co-doped film, the results also suggest strongly that BMPs play an important role in establishing long-range ferromagnetic order, as proposed by Coey *et al.*[8] A direct observation of BMP overlap is thus an overriding goal for further experimental studies.

The authors thank B. Normand for assistance. This work was supported by the MOST of China (Projects No. 2006CB601002 and No. 2006CB921301).

*qmzhang@ruc.edu.cn

[1] T. Dietl, H. Ohno, F. Matsukura, J. Cibert, and D. Ferrand, Science **287**, 1019 (2000).
[2] K. Sato and H. K. Yoshida, Jpn. J. Appl. Phys. **39**, L555 (2000); **40**, L334 (2001).
[3] K. Ueda, H. Tabata, and T. Kawai, Appl. Phys. Lett. **79**, 988 (2001).
[4] B. Martínez, F. Sandiumenge, L. I. Balcells, J. Fontcuberta, F. Sibieude, and C. Monty, J. Appl. Phys. **97**, 10D311 (2005).
[5] G. Lawes, A. S. Risbud, A. P. Ramirez, and R. Seshadri, Phys. Rev. B **71**, 045201 (2005).
[6] M. Bouloudenine, N. Viart, S. Colis, J. Kortus, and A. Dinia, Appl. Phys. Lett. **87**, 052501 (2005).
[7] S.-J. Han, J. W. Song, C.-H. Yang, S. H. Park, J.-H. Park, Y. H. Jeong, and K. W. Rhie, Appl. Phys. Lett. **81**, 4212 (2002); A. H. Slobodsky, V. K. Dugaev, and M. Vieira, Condens. Matter Phys. **3**, 531 (2002); R. Bouzerar, G. Bouzerar, and T. Ziman, Phys. Rev. B **73**, 024411 (2006).
[8] J. M. D. Coey, M. Venkatesan, and C. B. Fitzgerald, Nature Mater. **4**, 173 (2005).
[9] R. M. de la Cruz, R. Pareja, R. González, L. A. Boatner, and Y. Chen, Phys. Rev. B **45**, 6581 (1992); F. Vigué, P. Vennéguès, S. Vézian, M. Läugt, and J.-P. Faurie, Appl. Phys. Lett. **79**, 194 (2001); G. Brauer, W. Anwand, W. Skorupa, J. Kuriplach, O. Melikhova, C. Moisson, H. von Wenckstern, H. Schmidt, M. Lorenz, and M. Grundmann, Phys. Rev. B **74**, 045208 (2006).
[10] G. L. Liu, Q. Cao, J. X. Deng, P. F. Xing, Y. F. Tian, Y. X. Chen, S. S. Yan, and L. M. Mei, Appl. Phys. Lett. **90**, 052504 (2007).
[11] J. M. Calleja and M. Cardona, Phys. Rev. B **16**, 3753 (1977); R. Cuscó, E. Alarcón-Lladó, J. Ibáñez, L. Artús, J. Jiménez, B. Wang, and M. J. Callahan, *ibid.* **75**, 165202 (2007), and references therein.
[12] A. Kaschner, U. Haboeck, M. Strassburg, G. Kaczmarczyk, A. Hoffmann, C. Thomsen, A. Zeuner, H. R. Alves, D. M. Hof-

mann, and B. K. Meyer, Appl. Phys. Lett. **80**, 1909 (2002).
[13] C. Bundesmann, N. Ashkenov, M. Schubert, D. Spemann, T. Butz, E. M. Kaidashev, M. Lorenz, and M. Grundmann, Appl. Phys. Lett. **83**, 1974 (2003); N. Hasuike, H. Fukumura, H. Harima, K. Kisoda, H. Matsui, H. Saeki, and H. Tabata, J. Phys.: Condens. Matter **16**, S5807 (2004).
[14] F. J. Manjón, B. Marí, J. Serrano, and A. H. Romero, J. Appl. Phys. **97**, 053516 (2005); J. Serrano, A. H. Romero, F. J. Manjón, R. Lauck, M. Cardona, and A. Rubio, Phys. Rev. B **69**, 094306 (2004).
[15] V. G. Kravets, Phys. Rev. B **72**, 064303 (2005).
[16] G. H. Watson, Jr., W. B. Daniels, and C. S. Wang, J. Appl. Phys. **52**, 956 (1981).
[17] M. V. Wolkenstein, C. R. Acad. Sci. URSS **30**, 791 (1941).
[18] P. Umari, A. Pasquarello, and A. Dal Corso, Phys. Rev. B **63**, 094305 (2001).
[19] I. Bunget and M. Popescu, *Physics of Solid Dielectrics* (Elsevier Scientific, Amsterdam, 1984).
[20] W. Hayes and R. Loudon, *Scattering of Light by Crystals* (Wiley, New York, 1978).
[21] D. Gammon, R. Merlin, and H. Morkoc, Phys. Rev. B **35**, 2552 (1987).